Supplement of Hydrol. Earth Syst. Sci., 29, 7201–7216, 2025
https://doi.org/10.5194/hess-29-7201-2025-supplement

Hydrology and Earth System Sciences
Open Access

Supplement of

Microbial mats promote surface water retention in proglacial streams

Jonas Paccolat et al.

Correspondence to: Tom Battin (tom.battin@epfl.ch)

S1 Sediment texture

The size distribution of the fine and coarse sediments used during the flume experiments were measured by iteratively passing 500 g of sediments through seven sieves of mesh sizes 50 µm, 100 µm, 200 µm, 500 µm, 1000 µm, 2000 µm and 5000 µm and weighting the filtered material. The procedure was repeated three times and the mean value retained. The cumulative fractions were then fitted with the van Genuchten-like function

$$F(D) = \left(1 + \left(\frac{D}{D_g}\right)^N\right)^{-M}, \tag{S1}$$

where D is the particle size, D_g is a scale parameter and N and M are shape parameters related by the formula $M = 1 - 1/N$. Non-linear least squares fit (Fig. S1) yields $N = 3.8(2)$ and $D_g = 562(9)$ µm for the fine sediments and $N = 14.8(3)$ and $D_g = 1402(12)$ µm for the coarse sediments.

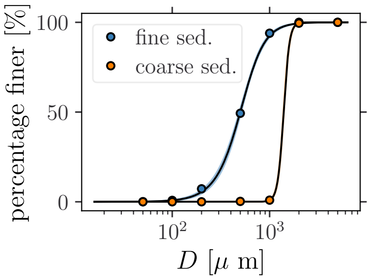

Figure S1: Cumulative particle size distribution of the fine and coarse sediments. The dots correspond to the sieving measurements, the black line to the best fit of Eq. (S1) and the shaded areas to the fit uncertainty obtained by varying the fit parameters over one standard deviation.

S2 Flume experiment

We present here the fitting procedure to estimate the sediment layer permeability, k_s, and the clogging layer permeability, k_c, form the flume experimental setup. The Python implementation is available from https://gitlab.com/jonas.paccolat/flume-monitor. The procedure is based on the assumption of a saturated column composed of two uniform layers: a sediment layer underlying a clogging layer. The permeability is thus k_s for $z \in [0, w_s]$ and k_c for $z \in [w_s, w_s + w_c]$, where w_s and w_c are the thickness of the sediment and clogging layers, respectively, and z is the vertical coordinate whose origin is at the bottom of the box. The sediment layer may be smaller than the actual sediment extent of height $L = 21$ cm to account for the potential interstitial clogging. Consequently $w_s = L - w_{\text{mix}}$ and $w_c = w_{\text{mix}} + w_{\text{mat}}$, where w_{mix} is the penetration depth of the clogging layer into the sediments and w_{mat} the mat thickness. It is assumed that the interstitial clogging and the surface clogging have identical permeability in agreement with the two-layers description. In reality, a continuous transition is expected within the sediments as well as within the mat itself because of microbial response to physico-chemical gradients. Consequently the permeability, k_c, should be understood as an effective quantity describing an equivalent uniform layer. It follows from the steady-state Darcy equation that the head profile is piece-wise linear with constant slope within each layer as represented on Fig. 2b of the main text. If $w_{\text{mat}} = 0$, the average box permeability is

$$k_0 = \frac{\nu}{g} \frac{q}{1 + (h^{\text{up}} - h^{\text{dn}})/L}, \tag{S2}$$

where h^{up} and h^{dn} are the imposed upper and lower pressure heads. The microbial mat thickness is interpolated from measurements using the logistic function

$$f(t) = \frac{w^\star}{1 + (w^\star/w_0 - 1)\exp(-t/\tau)}. \tag{S3}$$

Besides the best fit $w_{\text{mat}}^{\text{best}}(t)$, upper and lower limits, $w_{\text{mat}}^{\text{max}}(t)$ and $w_{\text{mat}}^{\text{min}}(t)$, are also obtained by varying each fit parameter ($w^\star$, w_0 and τ) within two standard deviations. Because of the uncertainty on w_{max} and our ignorance regarding the penetration depth w_{mix} both quantities are scanned, respectively from $w_{\text{mat}}^{\text{min}}$ to $w_{\text{mat}}^{\text{max}}$ and from 0 to $w_{\text{mix}}^{\text{max}}$. The latter bound is user-defined and set to $w_{\text{mix}}^{\text{max}} = 2$ cm by default. For $w_{\text{mat}} > 0$, the average box permeability is $k = k_0(1 + w_{\text{mat}}/L)$. For each pair of variables $(w_{\text{mat}}, w_{\text{mix}})$, the triangle fit (Fig.

S2) is applied to the pressure head profile h_P (list of the nine piezometers measurements). The upper pressure head $h^{\rm up}$ being the height difference between the water level and the sediment surface, a small correction must be accounted for in the presence of a microbial mat, such that $h(L + w_{\rm mat}) = h^{\rm up} - w_{\rm mat}$. To highlight the layering effect the linear trend is subtracted, i.e., $h_P^{(0)} = h^{\rm dn} + sz$, where $s = (h^{\rm up} - w_{\rm mat} - h^{\rm dn})/(L + w_{\rm mat})$. A positivity criterion is applied on the reduced pressure head profile $\delta h_P(z) = h_P^{(0)}(z) - h_P(z)$. If $\langle \delta h_P \rangle < \epsilon$, with ϵ a user-defined limit (set to $\epsilon = 1 \times 10^{-2}$ m by default), the profile is assumed uniform and the effect of the microbial mat is neglected. If however the criterion is fulfilled, the profile is assumed clogged and the two-layers model is suited. Fitting (with non-linear least squares) the triangle function

$$f_a(z, L, w_{\rm mix}, w_{\rm mat}) = \begin{cases} \delta s_1\, z, & \text{if } z < L - w_{\rm mix} \\ a + \delta s_2\,(z - L + w_{\rm mix}), & \text{otherwise} \end{cases}, \tag{S4}$$

with

$$\delta s_1 = \frac{a}{L - w_{\rm mix}} \quad \text{and} \quad \delta s_2 = -\frac{a}{w_{\rm mix} + w_{\rm mat}},$$

on the reduced pressure heads $\delta h_P(z)$ for given values of L, $w_{\rm mix}$ and $w_{\rm mat}$ yields estimates of the permeabilities of interests:

$$k_s = k\frac{1+s}{1+(s-\delta s_1)} \quad \text{and} \quad k_c = k\frac{1+s}{1+(s-\delta s_2)}. \tag{S5}$$

A weight is then assigned to each pair $(w_{\rm mat}, w_{\rm mix})$ according to the expression

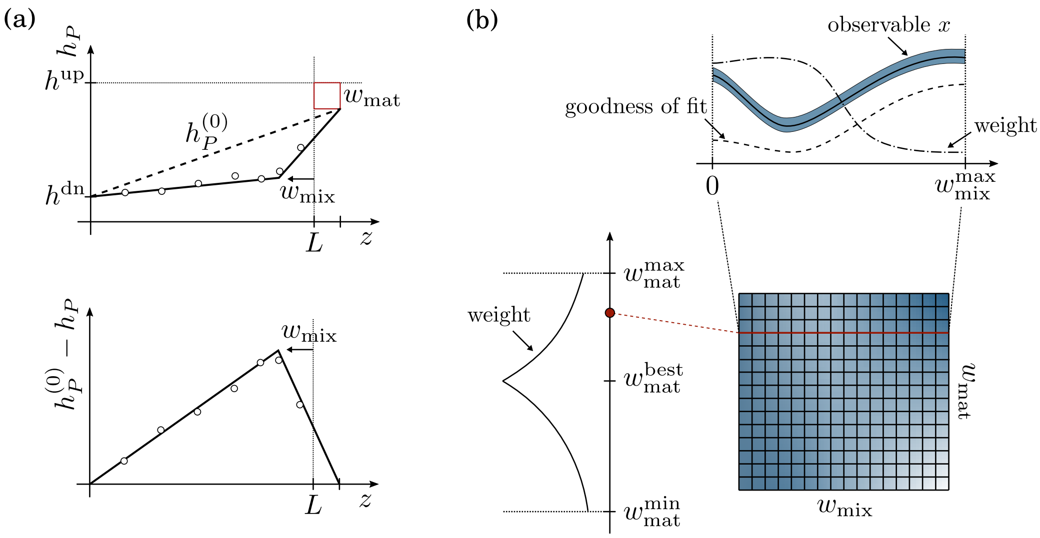

Figure S2: Illustration of the two-layers model fitting procedure. Both $w_{\rm mix}$ and $w_{\rm mat}$ are varied over a respective range of values as illustrated on (b). For each pair of value, the quantities k_s and k_c (generically represented by the blue landscape and the notation x on (b)) are computed according to the triangle fit illustrated on (a). A weight and goodness-of-fit is also associated to each grid point.

$$\rho(w_{\rm mat}, w_{\rm mix}) = \exp(-\frac{\rm gof}{{\rm gof}_{\rm cr}})\ \exp(-2\frac{|w_{\rm mat} - w_{\rm mat}^{\rm best}|}{w_{\rm mat}^{\rm max} - w_{\rm mat}^{\rm min}}), \tag{S6}$$

where the first term accounts for the fit quality through a chosen goodness-of-fit (gof) metric and the second term accounts for the distance to the best fit prediction $w_{\rm mat}^{\rm best}$. The root-mean-square error is used for the gof metric. The gof scale is a user-defined parameters set to ${\rm gof}_{\rm cr} = 3$ mm by default. This weight function is then used to compute the weighted average values $\langle k_c \rangle$ and $\langle k_s \rangle$, where the uncertainty is given by the maximum between the mean of the standard deviations and the standard deviation of the means. Finally, the penetration density function $\rho(w_{\rm mix})$ is obtained by averaging $\rho(w_{\rm mat}, w_{\rm mix})$ over the $w_{\rm mat}$ axis. This procedure is illustrated on Fig. S2. There are at least two replicates at each time-point associated to the two piezometer columns and potentially more if multiple values of $h^{\rm dn}$ have been considered. The weighted weight $\langle \rho \rangle$ is then used to average over the replicates. A simple average is applied to the histograms.

Concomitant to the mat permeability displayed on Fig. 2a of the main text, the associated sediment permeability, gof and weights are shown on Fig. S3. The histograms $\rho(w_{\rm mix})$ can be found in the repository. They merely indicate a uniform penetration likelihood between the sediment surface and the uppermost unclogged piezometer.

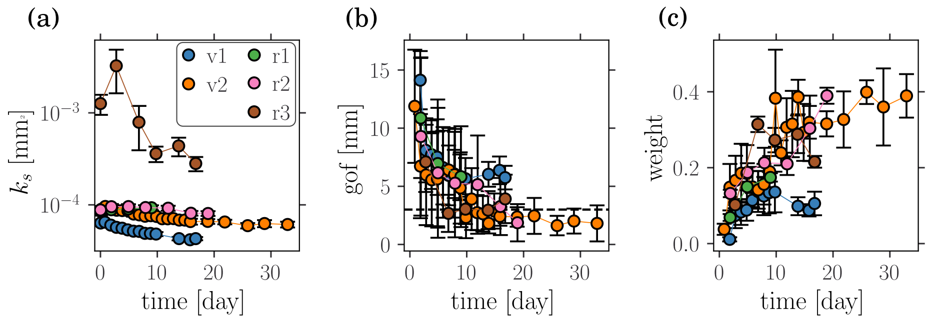

Figure S3: Time evolution of the (a) sediments permeability, (b) goodness-of-fit and (c) fit weight for all flume experimental runs. All quantities and uncertainties are estimated from the two-layers model and averaged over all replicates (left and right piezometer columns as well as the different pressure profiles monitored). The horizontal dashed lines on (b) correspond to the gof scale (i.e., 3 mm).

S3 Core experiments

Saturation protocol Hydraulic conductivity depends on the completeness of the sediment saturation (Klute & Dirksen, 1986). For dry sediments, full saturation is approached by flushing CO_2 into the sediment matrix to replace the air before slowly filling it with water from below. However, for initially wet sediments (as those sampled from the flume experiments or taken out of the oven) full saturation is impossible because CO_2 flushing is impracticable. Instead, *wet saturation* was obtained by applying a vacuum at the bottom of the tube (35 kPa, arbitrary but close to field capacity to avoid damaging the mat) for five minutes before letting water being sucked up to the sediment lower limit and then slowly increasing the water level until the top of the sediment columns. Air suction aims at minimizing air entrapment. Comparing both procedures, 3.1(1) % of air is nevertheless entrapped in the fine sediments. The hydraulic conductivity of the fine sediments following wet saturation is 70(10) % of fully saturated sediments (Fig. S4a). Because entrapped air dissolves in the water, the hydraulic conductivity increases over time, as observed on Fig. **??** for 20 °C well-aerated water. All replicates follow a similar linear trend, $k_{\mathrm{sed}}(t) = 47(8) \times 10^{-6} + 0.6t\,\mathrm{mm}^2$, where the uncertainty corresponds to twice the root-mean-square error.

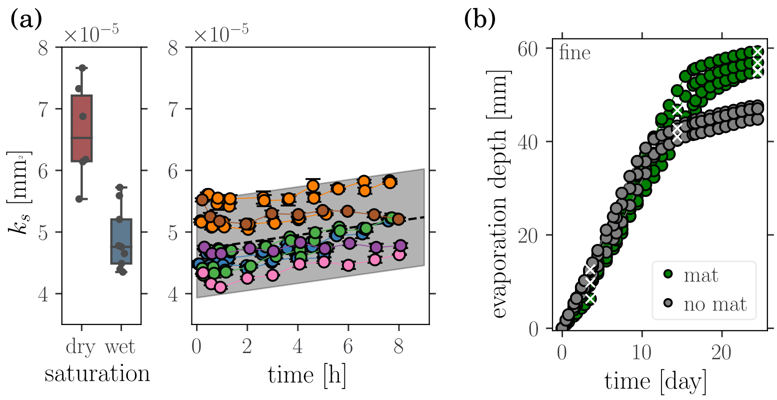

Figure S4: (a) Evolution of the permeability following wet saturation. A different colour is assigned to each replicate core. The same colour indicates that the same core was reused. The dashed line correspond to the linear fit $k_{\mathrm{sed}}(t) = 47 \times 10^{-6} + 0.6t\,\mathrm{mm}^2$ and the shaded area to the uncertainty $\Delta k = 8 \times 10^{-6}\,\mathrm{mm}^2$. (b) Evaporation curve of the nine core replicates samples at the end of *r2* together with three controlled cores without microbial mat. The white crosses indicate which and when cores were taken out of the oven to quantifiy the mat response to desiccation.

Evaporation experiments Evaporation from porous media is characterized by two phases (see Lehmann et al. (2008) and reference therein). In stage I, the evaporation rate e ($\mathrm{m\,s^{-1}}$) is roughly equal to the potential evaporation rate e_0 of a water pan, which is controlled by atmospheric demand. It results in a drying front propagating downward at constant velocity. The air first penetrates the largest pores leaving the smallest one water saturated. When the drying front reaches a critical depth, flow connectivity breaks down as a dry layer forms at the surface. Stage II of evaporation is thus diffusion limited which translates into a decaying evaporation rate. Nine core replicate were sampled at the end of *r2*, resaturated (wet procedure) and put in an oven at 30 °C together with three control cores without microbial mat. The atmospheric pressure and the relative humidity in the oven were continuously monitored; in average they were respectively 961(4) Pa and 49(5) %. All tubes were weighted every day for 25 days to measure the evaporation curve (Fig. S4b). The critical evaporation depth E_c corresponding to the end of stage I was significantly larger in the presence of microbial material (Welch's t-test: $t = 3.4$, $df = 7.8$, $p = 0.01$).

References

Klute, A., & Dirksen, C. (1986). Hydraulic Conductivity and Diffusivity: Laboratory Methods. In *Methods of Soil Analysis* (pp. 687–734). John Wiley & Sons, Ltd. https://doi.org/10.2136/sssabookser5.1.2ed.c28

Lehmann, P., Assouline, S., & Or, D. (2008). Characteristic lengths affecting evaporative drying of porous media. *Physical Review E*, *77*(5), 056309. https://doi.org/10.1103/PhysRevE.77.056309